Characteristics of Transparent, PEDOT:PSS Coated Indium-Tin-Oxide (ITO) Microelectrodes

Weiyang Yang, Allison Broski, Jiajia Wu, Qi Hua Fan and Wen Li, Senior *Member, IEEE*

***Abstract* —This paper reports on electrochemical and optical characteristics of flexible, transparent microelectrodes, which consist of thin poly-(3, 4-ethylenedioxythiophene)/poly(styrenesulfonate) (PEDOT:PSS) spun onto indium-tin-oxide (ITO) electrodes for potential applications in biomedical optoelectronic devices. Although PEDOT:PSS/ITO combined films have been extensively investigated for applications in optical devices, such as solar cells and LEDs, PEDOT:PSS/ITO films for use in electrophysiological recording have not been well-characterized yet. In this work, PEDOT:PSS coated ITO microelectrodes with various diameters of 10 µm, 37 µm, 50 µm and 80 µm were microfabricated and characterized, and their properties were compared with plain ITO microelectrodes. Experimental results demonstrate that PEDOT:PSS coated ITO electrodes exhibit decreased electrochemical impedance, well-performed stability in saline, and increased charge storage capacity while preserving excellent optical transparency and mechanical flexibility. Equivalent circuit models were fitted to the experimental results to analytically extract interface capacitance, charge transfer resistance and solution resistance at the electrode-electrolyte interface.**

***Index Terms* — Indium-tin-oxide, PEDOT:PSS, transparent microelectrodes, biomedical optoelectronic devices.**

I. Introduction

Optogenetics is a revolutionary neuromodulation technique that utilizes light to excite or inhibit the activity of genetically targeted neurons, expressing light-sensitive opsin proteins [1]. To fully realize the potential of the optogenetics tools, neural interface devices with both recording and stimulating capabilities are vital for future engineering development, and improving their spatial precision is a topic of constant research. While ITO has been used in making transparent recording microelectrodes for optogenetics applications [2], it contains expensive rare elements and has poor mechanical flexibility. Moreover, ITO electrodes, when scaled down to micron dimensions, face a critical problem of an increased electrochemical impedance, which would lead to undesirable electrochemical reactions with the brain tissue [3] and poor recording quality due to noisy, ion-based electric fluctuations of the surrounding media [4]. Thus, there is an urgent need to develop low-impedance, transparent microelectrodes as a neural recording interface in combination with optogenetics. PEDOT:PSS, as one of the most prevalent conducting polymers (CPs), has been demonstrated with many desirable properties for electrophysiological recording, including high biostability, outstanding biocompatibility, and simple utilization with low-cost spin-coating and ink-jet printing techniques [5-6]. However, PEDOT:PSS has seldom been used independently as a transparent electrode because of its limited electrical conductivity. PEDOT:PSS can only achieve a sheet resistance of ~40 ohms/sq even when doped with solvents, such as H_2SO_4, which is significantly higher than the ITO sheet resistance of ~10 ohms/sq [7].

To address the above challenges, we proposed a combined ITO-PEDOT:PSS electrode configuration by spinning thin PEDOT:PSS films on ITO microelectrodes, for applications in low-impedance neural recordings. PEDOT:PSS coated ITO microelectrodes with different diameters were microfabricated and characterized experimentally, and their properties were compared with plain ITO microelectrodes. In particular, electrochemical impedance spectroscopy (EIS) was used to analyze the frequency-dependent impedance of the microelectrodes in a 0.9% NaCl (saline) solution. Equivalent circuit models were applied to fit the experimental results into parameters representing macroscopic physical quantities related to electrode-electrolyte interface impedance. Cyclic voltammetry (CV) was used to quantify the charge storage capacity of the microelectrodes. Atomic force microscopy (AFM) and ultraviolet-visible (UV-Vis) spectroscopy were used to study the sample's surface morphology and optical transmittance, respectively.

II. Method

A. Design and fabrication of microelectrode probes

Each probe under test consisted of 6 transparent microelectrodes distributed uniformly along the tip of a single shank, and interconnection wires and contact pads made out of copper (Fig. 1a). To fabricate the ITO electrode probe, first, 500 nm copper was thermally evaporated (Edward Auto306, Edwards, UK) on an ITO coated polyethylene terephthalate (PET) substrate (639303, Sigma-Aldrich). The copper was patterned using ultraviolet (UV) photolithography and then etched in copper etchant. Next, photoresist (PR) was spun on the substrate and photolithographically patterned to form a mask for chemical etching of ITO in 5% hydrochloric acid. After ITO electrodes were constructed, 2 µm Parylene-C was deposited (PDS 2010, Specialty Coating System, Inc) on the substrate as an insulation layer. Then Parylene-C on the contact pads and ITO electrodes was removed completely using oxygen plasma dry etching (RIE-1701 plasma system, Nordson March, Inc). Prior to PEDOT:PSS coating, a PR mask was patterned to expose only the ITO electrode

Manuscript received August 30, 2017. This work was supported in part by National Institutes of Health under Award NIH R21NS096637-02 and Michigan State University Strategic Partnership Grants.

Weiyang Yang, Jiajia Wu, and Wen Li are with the Microtechnology Laboratory; Qi Hua Fan is with the Plasma Sources and Processing Laboratory, Department of Electrical and Computer Engineering, Michigan State University, East Lansing, MI, 48824 USA (email: yangweiy@msu.edu; wujiaji1@msu.edu; qfan@msu.edu; wenli@egr.msu.edu).

Allison Broski is with Oakland University, Rochester, MI, USA (email: broski.ac@gmail.com).

Color versions of one or more of the figures in this paper are available online at http://ieeexplore.ieee.org.

Digital Object Identifier XXXXXXXXXXXXXXXX

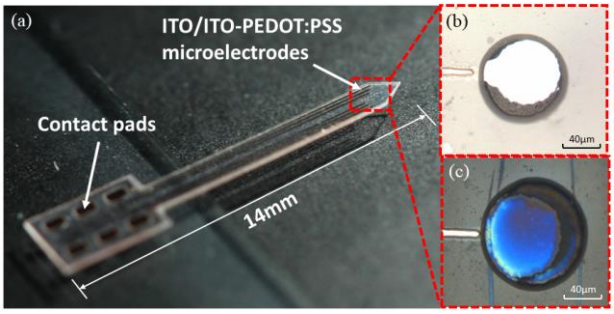

Fig. 1. (a) Photo of a fabricated microelectrode probe. Microscope images of the ITO electrodes without (b) and with PEDOT:PSS coating (c).

sites. PEDOT:PSS (768642, Sigma-Aldrich) was spun on the top of the substrate with 500 rpm spin speed for 30 secs and then 4000 rpm for 120 secs, followed by baking on a hotplate at 100ºC for 30 mins. Finally, PR was rinsed off with acetone, isopropyl alcohol (IPA) and deionized (DI) water to remove unwanted PEDOT:PSS, leaving PEDOT:PSS on top of the ITO microelectrodes. Fig. 1 (b) and (c) show examples of the fabricated ITO microelectrodes before and after the PEDOT:PSS treatment.

B. *Testing Methods*

To fully understand the electrochemical properties of the transparent microelectrodes, EIS measurements were performed using a potentiostat (Electrochemical Analyzer, CH Instruments, Inc.) in a three-electrode cell [8], with the ITO or PEDOT:PSS coated ITO microelectrode as the working electrode (WE), an Ag/AgCl electrode as the reference electrode (RE), and a platinum electrode as the counter electrode (CE). The tests were conducted in physiological saline solution at room temperature. The electrochemical impedance of the microelectrode was measured from 0.1 Hz to 100 kHz when a 5 mV RMS sinusoid waveform was applied to the WE. Using the above three-electrode setup, cyclic voltammograms (CV) of the microelectrode were measured at a 100 mV/s sweep rate in a potential range of -0.9 V to 0.9 V. Multiple CV scans were done in experiments before data collection to clean the electrode surface and allow the system to settle. Besides electrochemical measurements, an atomic force microscope (AFM) (5100N, Hitachi, Inc) was used to compare the surface microphology of the ITO microelectrodes with and without the PEDOT:PSS coating. Thin film optical transmittance was quantified by UV-Vis spectroscopy (Lambda 900, Perkin Elmer) in a wavelength range of 310-750 nm. The PEDOT:PSS film thickness was measured by a profilometer (Nanomap-500LS, Aeptechnology, Inc.), and the sheet resistance of the pure ITO and PEDOT:PSS coated ITO films was detected by a four-point probe station (Lucas Signatone SP4, Signatone).

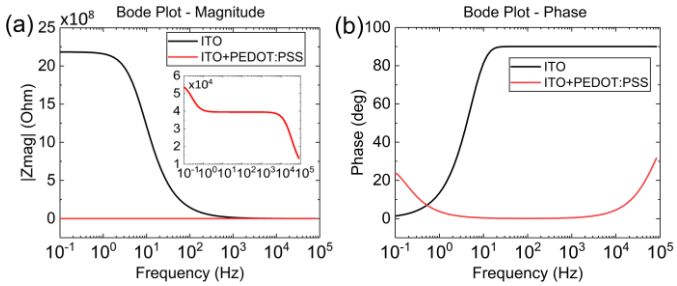

Fig. 2. (a) Impedance modulus and (b) phase versus frequency for plain ITO and PEDOT:PSS coated ITO microelectrodes, respectively.

III. Results and Discussion

A. *Impedance*

The average thickness of the PEDOT:PSS coating was 103 nm (n=5). The sheet resistance was 59.96 ohm/sq and 56.35 ohm/sq (n=5) for the PEDOT-PSS coated ITO and pure ITO film, respectively, which were consistent with the values provided by Sigma-Aldrich. The PEDOT:PSS coated ITO film exhibits a slightly higher resistance than the pure ITO film. For the EIS measurements, four different diameters of the ITO electrodes with and without the PEDOT:PSS coating were tested: 10 μm, 37 μm, 50 μm and 80 μm. These diameters were chosen to match the size of neuron cell body for single unit recording, which typically varies from 4 μm to 100 μm in diameter [9]. The Bode plots in Fig. 2 (a) and (b) show the typical electrode impedance magnitude and phase versus frequency, respectively. The impedance of the PEDOT:PSS coated ITO electrode was highly resistive over a wide frequency range of 1 Hz – 10 kHz, suggesting that charge transfer is attributed to reversible faradaic reactions. The PEDOT:PSS coating effectively reduced the overall electrochemical impedance of the microelectrodes in a wide frequency spectrum, in consistence with other reports [10]. Fig. 3 (a) showed that the average impedance at 1 kHz decreased when the electrode area increased for both the plain and PEDOT:PSS coated ITO microelectrodes. The impedances of the PEDOT:PSS coated microelectrodes were consistently two orders of magnitude lower than those of the plain ITO microelectrodes.

This reduction in impedance is mainly attributed to the increase in the surface roughness of the microelectrodes after the PEDOT:PSS coating, as indicated in the AFM images in Fig. 4. The average roughness (R_a) and peak-to-peak mean roughness depth (R_t) of the PEDOT:PSS-ITO film is 3.33 nm and 39.15 nm, respectively, while R_a and R_t of the ITO film is 0.85 nm and 12.02 nm, respectively. The rough surface provides a large effective surface area of the electrode when exposed to the

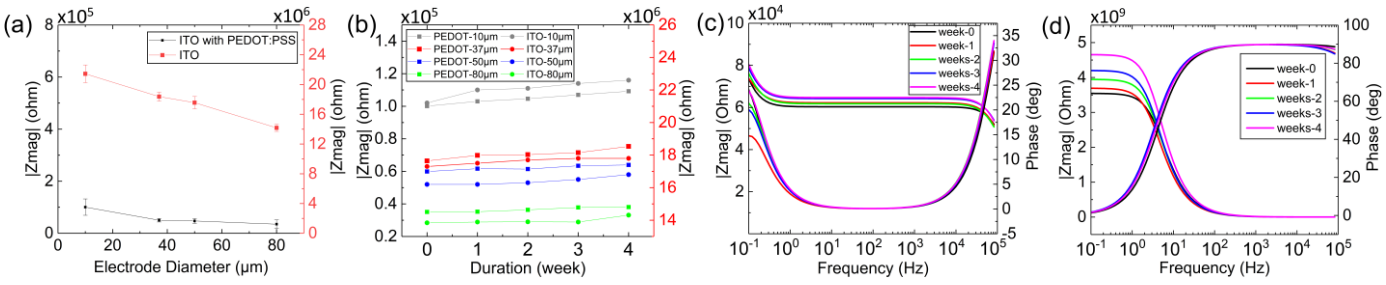

Fig. 3. (a) Average 1 kHz impedance of the plain and PEDOT:PSS coated ITO microelectrodes with 10 μm, 37 μm, 50 μm and 80 μm diameters (n=5). (b) Impedance changes of the pure ITO and PEDOT:PSS coated ITO electrodes with different diameters, measured after soaked in room temperature saline for 0 weeks, 1 week, 2 weeks, 3 weeks and 4 weeks. Impedance magnitude (upper curves, high-to-low curves) and phase changes (lower curves, low-to-high curves) during 4 weeks for the PEDOT:PSS coated ITO microelectrodes (c) and for the pure ITO electrodes (d).

electrolyte, allowing more charge to flow across the electrode-electrolyte interface. Consequently, the PEDOT:PSS coating reduced the electrode's impedance.

To evaluate the stability of the microelectrodes, the devices were kept in saline at room temperature for up to 4 weeks, and their impedance and phase changes were monitored weekly and plotted in Fig. 3 (b), (c) & (d). Our results show that the PEDOT:PSS coated ITO electrodes exhibited good stability over four weeks with an overall impedance increase of less than 7.23%, which is slightly higher than the ITO electrodes (with an impedance increase of 3.62%). The increase in impedance magnitude may be due to PEDOT:PSS reaction with oxygen and moisture. PEDOT:PSS absorbs water upon exposure to air, creating an aqueous acid environment that facilitates etching of the ITO [11]. Indium etch products will then be transported throughout the PEDOT:PSS film, thereby weakening the stability of the ITO-PEDOT:PSS interface and slowly increasing impedance. The impedance magnitude of week 2 was slightly lower than week 1, possibly because the Parylene-C layer was a little detached from the substrate, leading to more ITO electrode exposure in the saline solution during the electrochemical testing which counteracted the influence from oxygen and moisture. Of note is that exposing the device to saline had minimal impact on the impedance phase within the frequency range of interest (100 Hz – 10 kHz) [12]. Visual inspection did not observe any signs of major physical damage and delamination of the PEDOT:PSS coating.

B. Charge Storage Capacity

Fig. 5 (a) plots the CV scans of both the plain and PEDOT:PSS coated ITO electrodes. For the PEDOT:PSS coated devices, the larger area under the CV curve indicates a larger cathodic charge storage capacity, as compared to the plain ITO electrode. The charge storage capacity of the electrodes calculated from these CV curves was 58.06 $\mu C/cm^2$ for the plain ITO electrode and 582.45 $\mu C/cm^2$ for the PEDOT:PSS coated ITO electrode. Our result is consistent with those from previous studies [13], where PEDOT:PSS films had been proven to have a large degree to enhance the charge storage capacity due to the increased effective surface area. Fig. 5 (b) shows the CV scans of the PEDOT:PSS coated electrode for 10 consecutive cycles, indicating the excellent short-term stability of the PEDOT:PSS coating in room temperature saline solution.

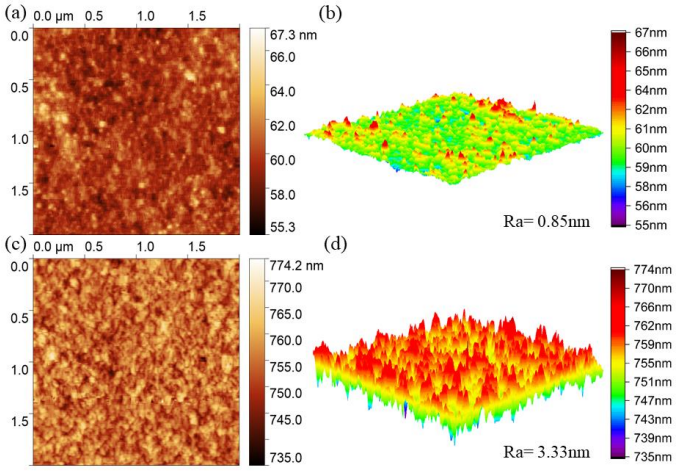

Fig. 4. AFM images of the plain ITO substrate (a) & (b), and the PEDOT:PSS coated ITO substrate (c) & (d).

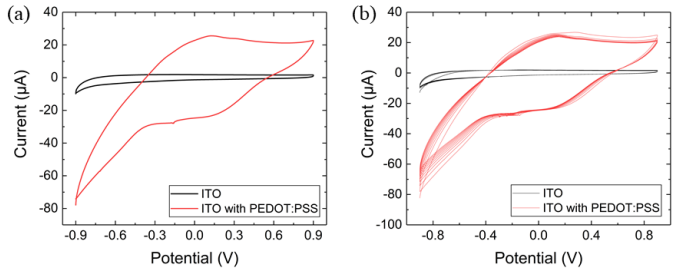

Fig. 5. (a) CVs of the plain ITO and PEDOT:PSS coated ITO WEs versus Ag/AgCl RE, showing that the PEDOT:PSS coated ITO electrode exhibits larger charge storage capacity. (b) CVs of the plain ITO and PEDOT:PSS coated electrode for 10 cycles, demonstrating the stability of the ITO and the PEDOT:PSS coating in saline.

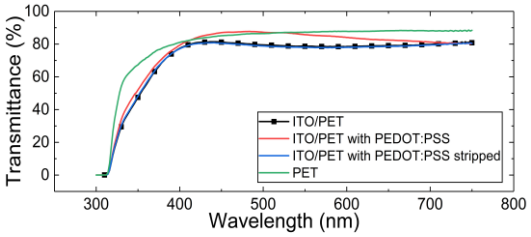

Fig. 6. Optical transmittance of different thin films.

C. Optical Transmittance

Fig. 6 shows the optical transmittance of different substrates: pure PET, ITO/PET, ITO/PET with PEDOT:PSS, and ITO/PET with PEDOT:PSS stripped. It can be seen that the PEDOT:PSS coating significantly improves the optical transmittance throughout the visible range of 400-700 nm. Because the refractive index of the PEDOT:PSS (1.334) is much smaller than that of the ITO (1.972), the overall reflective loss at the air-PEDOT:PSS and PEDOT:PSS-ITO interface is lower than that at the air-ITO interface, based on the Fresnel equations [14]. Since PEDOT:PSS has a very small absorption coefficient in UV-Vis region [15], the transmittance improvement of the PEDOT:PSS coated ITO is mainly attributed to the decrease in reflectance at the air-substrate interface. A quarter-wave effect may also contribute to the increase in transmittance: $nd = \lambda/4$, where n and d is the refractive index and thickness of the film, respectively, and λ is the wavelength [14]. At visible wavelengths, the thickness of our PEDOT:PSS film (103 nm) fits the quarter-wave situation, where the PEDOT:PSS film acts as an antireflective layer, allowing more light to be transmitted through the substrate. Both the PEDOT:PSS coated ITO and pure ITO films show strong absorption at 310-400 nm.

D. Equivalent Circuit Model

We studied the physical processes contributing to the electrode impedance using equivalent circuit models. The circuit model in Fig. 7 (a) obtained from [16] was used for the plain ITO electrode, which consists of a constant phase angle impedance Z_{CPA}, shunted by a charge-transfer resistance R_c, in series with the solution resistance R_s. After the ITO surface was covered with PEDOT:PSS, the device was modeled by the circuit in Fig. 7 (b), where an additional Z_{CPA}-R_c circuit element was used. The first Z_{CPA}-R_c parallel element represents the electron transfer occurring at the ITO-PEDOT:PSS interface while the second Z_{CPA}-R_c element represents the charge transfer reaction at the PEDOT:PSS-electrolyte interface. The two parallel circuit elements were put in series with the solution resistance R_s. The Warburg impedance was not included in this study because it did not have a significant contribution to the overall impedance in our experiment

Table 1. SUMMARY OF THE FITTED VALUES BY UTILIZING THE EQUIVALENT CIRCUIT MODELS

Materials	Diameter [μm]	Z_{CPA1} [Ohm]	R_{C1} [Ohm]	Z_{CPA2} [Ohm]	R_{C2} [Ohm]	R_S+R_W [Ohm]	Total Impedance
ITO	80	4.67E+10	1.25E+10	——	——	1.34E+04	9.86E+09
	50	8.61E+10	1.14E+10	——	——	1.19E+04	1.01E+10
	37	9.06E+10	1.17E+10	——	——	2.49E+04	1.03E+10
	10	9.34E+10	2.88E+10	——	——	1.52E+04	2.20E+10
ITO-PEDOT:PSS	80	3.54E+10	3.53E+04	6.08E+04	1.04E+04	1.88E+04	6.29E+04
	50	3.04E+10	4.16E+04	1.66E+04	3.67E+04	2.26E+04	7.56E+04
	37	4.23E+10	4.97E+04	1.57E+04	2.67E+04	1.62E+04	7.59E+04
	10	3.27E+10	5.77E+04	2.55E+04	2.86E+04	1.53E+04	8.64E+04

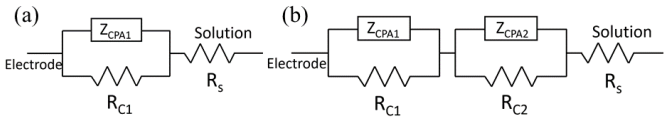

Fig. 7. Equivalent circuit model of (a) the pure ITO and (b) the ITO-PEDOT:PSS electrode-electrolyte interface.

[17]. The constant phase angle impedance, which is a measure of the non-faradaic impedance, can be calculated by the empirical relation:

$$Z_{CPA}(\omega) = \frac{1}{(j\omega Q)^n} \qquad (1)$$

where Q is a measure of the magnitude of Z_{CPA}, n is a constant ($0 \leq n \leq 1$) representing inhomogeneity in the surface, and $\omega = 2\pi f$. When $n = 1$, Z_{CPA} corresponds to an interface capacitance that acts as a purely capacitive impedance element [4]. The solution resistance R_s is the resistance between the working electrode and the reference electrode. The charge transfer resistance arises from the low-field approximation of the Butler-Volmer equation, which reduces to Ohm's law.

Table 1 shows the fitted values based on the above models. The impedances of the interface capacitance were calculated using Eq. 1 at an angular frequency of 1 s^{-1}. The fitted parasitic resistance is given as $R_s + R_w$, where R_w is the resistance of the wire connecting the electrode to the testing instrument. Finally, we calculated the overall impedances of each microelectrode. The results show that the PEDOT:PSS coating leads to a decrease in R_c by 6 orders of magnitude at both the ITO-PEDOT:PSS and PEDOT:PSS-solution interfaces. Compared to the ITO-electrolyte interface, the PEDOT:PSS-electrolyte interface exhibited much lower Z_{CPA} values, which were comparable to the reduced R_c values. Consequently, the total impedance magnitude of the PEDOT:PSS coated ITO microelectrode was 6 orders smaller than that of the plain ITO microelectrode. These analytical results for the PEDOT:PSS coated ITO have not been well-concluded in electrophysical recording before our investigation, while the solar cells and LEDs have been extensively-researched [18].

IV. Conclusion

In this paper, we fully characterized the electrochemical properties of the PEDOT:PSS coated ITO microelectrodes, which exhibit significantly improved impedance and charge capacitance over the pure ITO electrodes, suitable for use in neurophysiological recording. The PEDOT:PSS coated ITO electrodes remain stable over 4 weeks in room temperature saline. The PEDOT:PSS coating results in a rougher surface microphology, which contributes to the impedance decrease and capacitance increase of the electrode. The EIS results were fitted into the equivalent circuit models, confirming that the significantly reduced impedance of the electrode was caused by the PEDOT:PSS coating. Lastly, the PEDOT:PSS coating improves the optical transmittance in the visible spectrum by reducing the reflectance at the air-substrate interface. Future work will focus on evaluating electrode functionality in *in vivo* neural recording experiments.

Reference

[1] G. Nagel, T. Szellas, W. Huhn, S. Kateriya, N. Adeishvili, P. Berthold, D. Ollig, P. Hegemann and E. Bamberg, "Channelrhodopsin-2, a directly light-driven selective membrane channel," *Proc. Natl. Acad. Sci. U. S. A.*, vol. 100, pp. 13940–13945, 2003.

[2] K. Y. Kwon, B. Sirowatka, A. Weber, and W. Li, "Opto-μECoG array: A hybrid neural interface with transparent μECoG electrode array and integrated LEDs for optogenetics." *IEEE Trans. Biomed. Circuits Syst.*, 7.5 pp. 593-600, 2013.

[3] M. O. Heuschkel, "Fabrication of multi-electrode array devices for electrophysiological monitoring of in-vitro cell/tissue cultures." In Series in Microsystems, P.A. Besse, M. Gijs, R.S. Popovic, and Ph. Renaud Eds. Konstanz, Germany: Hartung-Gorre, vol.13, 2001.

[4] W. Franks, I. Schenker, P. Schmutz, and A. Hierlemann, "Impedance characterization and modeling of electrodes for biomedical applications, " *IEEE Trans. Biomed. Eng.*, vol. 52, pp. 1295-1302, 2005.

[5] L. Groenendaal, G. Zotti, P. H. Aubert, S. M. Waybright, and J. R. Reynolds, "Electrochemistry of Poly (3, 4-alkylenedioxythiophene) Derivatives Advanced Materials," *Adv. Mater.*, vol.15, pp. 855-879, 2003.

[6] S. Venkatraman, J. Hendricks, Z. A. King, A. J. Sereno, S. Richardson-Burns, D. Martin, and J.M. Carmena, "In vitro and in vivo evaluation of PEDOT microelectrodes for neural stimulation and recording," *IEEE Trans. Neural Syst. Rehabil. Eng.*, vol. 19, pp. 307-316, 2011.

[7] X. Guo, X. Liu, F. Lin, H. Li, Y. Fan, and N. Zhang, "Highly conductive transparent organic electrodes with multilayer structures for rigid and flexible optoelectronics,"*Sci. Rep.*, vol. 5, 2015.

[8] M. C. Tsai, P. Y. Chen, "Voltammetric study and electrochemical detection of hexavalent chromium at gold nanoparticle-electrodeposited indium tin oxide (ITO) electrodes in acidic media," *Talanta*, vol. 76, pp. 533-539, 2008.

[9] A. Al-chalabi, R. S. Delamont and M. R. Turner, *The Brain: A Beginner's Guide*. Oxford, England: Oneworld Publications, 2008, pp. 181-183.

[10] A. A. Guex, N. Vachicouras, A. E. Hight, M. C. Brown, D. J. Lee and S. P. Lacour, "Conducting polymer electrodes for auditory brainstem implants," *J. Mater. Chem. B*, vol. 3, pp. 5021-5027, 2015.

[11] M. P. De Jong, L. J. Van Ijzendoorn, and M. J. A. De Voigt. "Stability of the interface between indium-tin-oxide and poly (3, 4-ethylenedioxythiophene)/poly (styrenesulfonate) in polymer light-emitting diodes," *Appl. Phys. Lett.*, vol. 77, pp. 2255-2257, 2000.

[12] B. Gosselin, A. E. Ayoub, J. F. Roy, M. Sawan, F. Lepore, A. Chaudhuri and D. Guitton, "A mixed-signal multichip neural recording interface with bandwidth reduction," *IEEE Trans. Biomed. Circuits Syst.*, vol. 3, pp. 129-141, 2009.

[13] D. Zhao, Q. Zhang, W. Chen, X. Yi, S. Liu, Q. Wang, Y. Liu, J. Li, X. Li and H. Yu, "Highly Flexible and Conductive Cellulose-Mediated PEDOT: PSS/MWCNT Composite Films for Supercapacitor Electrodes," *ACS Appl. Mater. Interfaces*, vol. 9, pp. 13213-13222, 2017.

[14] H. A. Macleod, *Thin-film optical filters*. Tucson, AZ, USA: CRC Press, 2009, pp. 23-215.

[15] J. Gasiorowski, R. Menon, K. Hingerl, M. Dachev and N. S. Sariciftci, "Surface morphology, optical properties and conducticity changes of poly (3, 4-ethylenedioxythiophene): poly (styrenesulfonate) by using additives," *Thin Solid Films*, vol. 536, pp. 211-215, 2013.

[16] G. T. A. Kovacs, "Introduction to the theory, design, and modeling of thin-film microelectrodes for neural interfaces," *Enabling technologies for cultured neural networks*, pp. 121–165, 1994.

[17] H. Hillebrandt, M. Tanaka, "Electrochemical Characterization of Self-Assembled Alkylsiloxane Monolayers on Indium− Tin Oxide (ITO) Semiconductor Electrodes," *J. Phys. Chem. B*, vol. 105, pp.4270-4276, 2001.

[18] M. P. De Jong, L. J. Van Ijzendoorn and M. J. A. De Voigt, "Stability of te interface between indium-tin-oxide and poly(3,4-ethylenedioxythiophene)/poly(styrenesulfonate) in polymer light-emitting diodes," *Appl. Phys. Lett.*, vol. 77, pp. 2255-2257, 2000.